

Fermilab-pub-07-413

MINOS-doc-3412

August 10, 2007

Preliminary Results from MINOS on  $\nu_\mu$  Disappearance Based on an  
Exposure of  $2.5 \times 10^{20}$  120 GeV Protons on the NuMI Target

The MINOS Collaboration

Submitted to the XXIII International Symposium  
on Lepton and Photon Interactions at High Energy,  
Daegu Korea, August 13–18, 2007.

### Abstract

Updating our previous measurements with new data and analysis modifications, we report preliminary results on the energy-dependent deficit of muon-neutrinos from the Fermilab NuMI beam as observed with the MINOS Far Detector located 735 km away in the Soudan Underground Laboratory. From an exposure of  $2.50 \times 10^{20}$  protons on target, we observe 563 charged-current  $\nu_\mu$  interaction candidates in the Far Detector, where  $738 \pm 30$  events are expected in the absence of neutrino oscillations. We have analyzed these data assuming two-flavor  $\nu_\mu \rightarrow \nu_\tau$  oscillations. From a simultaneous fit to the reconstructed  $\nu_\mu$  energy spectra obtained during two running periods we obtain the neutrino squared-mass difference  $\Delta m_{32}^2 = (2.38^{+0.20}_{-0.16}) \times 10^{-3} \text{ eV}^2/c^4$  with errors at 68% confidence level (CL), and mixing angle  $\sin^2(2\theta_{23}) > 0.84$  at 90% CL. The uncertainties and confidence intervals include both statistical and systematic errors. All results and plots presented here are *preliminary*.

## 1 Introduction

The MINOS Experiment was designed to explore the phenomenon of  $\nu_\mu$  disappearance as observed in experiments studying atmospheric neutrinos [1, 2, 3] and more recently in the K2K accelerator-based experiment [4]. The leading hypothesis for this phenomenon is neutrino oscillations, with  $\nu_\mu \rightarrow \nu_\tau$  the likely dominant oscillation mode. MINOS makes use of a configurable intense neutrino source (NuMI) derived from 120 GeV protons extracted from the Fermilab Main Injector onto a graphite target, and two magnetized-iron and scintillator detectors: a 0.98 kton Near Detector (ND) located on the Fermilab site approximately 1 km downstream of the NuMI target and a 5.4 kton Far Detector (FD) located in the Soudan Underground Laboratory at a distance of 735 km. The NuMI beam line and the MINOS detectors are described in detail elsewhere [5, 6].

In Ref. [7] we reported results based on data accumulated during the first period of NuMI operations between May 2005 and February 2006. We denote this period as ‘Run-I’. Far Detector data collected with the target in the ‘low-energy’ (LE) beam configuration, corresponding to an exposure of  $1.27 \times 10^{20}$  protons on target (POT), were analyzed in the

context of two-flavor  $\nu_\mu \rightarrow \nu_\tau$  oscillations. Oscillation parameters were obtained from a fit to the reconstructed charged-current (CC)  $\nu_\mu$  energy spectrum:  $\Delta m_{32}^2 = (2.74^{+0.44}_{-0.26}) \times 10^{-3} \text{ eV}^2/c^4$  for the squared-mass difference and  $\sin^2 2\theta_{23} = 1.00_{-0.13}$  for the mixing angle, where only the physical region  $\sin^2 2\theta_{23} \leq 1$  was considered and where the uncertainties represent approximate 68% confidence level (CL) intervals.

Following the Fermilab accelerator complex shutdown in spring 2006, NuMI resumed operations in June 2006. The period from then through July 2007 is referred to as ‘Run-II’. With some modifications relative to that reported in Ref. [7], we have carried out an analysis of the LE Run-I data plus the portion of the LE Run-II data collected through March 2007 (denoted as Run-IIa), corresponding to a combined exposure of  $2.50 \times 10^{20}$  POT. In this conference contribution, we report preliminary results on  $\nu_\mu$  disappearance from this analysis of Run-I and Run-IIa data.

## 2 Summary of Analysis Steps

Most aspects of the analysis follow those described in Ref. [7]. Briefly,  $\nu_\mu$  CC interactions candidates are selected from events in Near and Far Detector data samples with a reconstructed negatively charged muon. We employ the reconstructed  $\nu_\mu$  energy ( $E_\nu$ ) spectrum from the ND sample to obtain a prediction for the corresponding spectrum at the FD in the absence of oscillations. The extrapolation of the ND spectrum to the FD accounts for the kinematic and geometrical effects that impart small (up to  $\pm 30\%$ ) differences in shape between the two spectra. We carry out a binned maximum-likelihood fit of the FD spectrum to the oscillation probability-weighted prediction, incorporating major systematic uncertainties via penalty factors. The FD data was intentionally obscured during the analysis until all selection, fitting and systematic error estimation procedures were finalized.

The new analysis reported here, including updated results from the Run-I data, incorporates several improvements compared to our published analysis. The most significant improvements are:

- use of an upgraded neutrino interaction simulation package [8] that features more accurate models of hadronization, intranuclear rescattering and deep inelastic scattering processes. The combined effect of adopting the new hadronization and intranuclear rescattering models is a downward shift in the effective absolute energy scale of the MINOS detectors for hadronic showers from neutrino interactions by amounts varying from approximately 10% at 2 GeV to 5% at higher shower energies.
- a new track reconstruction algorithm, which results in a 4% increase in muon track reconstruction and fitting efficiency.
- increased acceptance achieved by including events with reconstructed  $E_\nu$  above 30 GeV (corresponding to a 9.6% expected increase in event yield), and by expanding the fiducial volume definition along the beam direction for the FD by 3.2%.

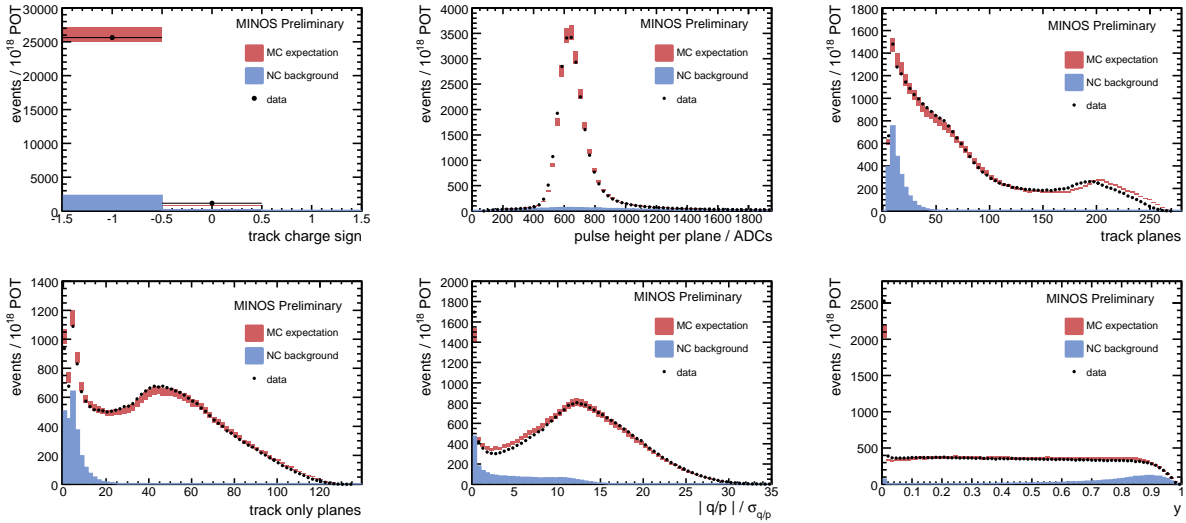


Figure 1: Input observables to the likelihood-ratio discriminant used for CC/NC event separation are shown for ND events in data (points) and MC (red bands). The expected NC background contribution shown by the shaded histograms. From upper left: track charge sign, average track pulse height per plane, number of planes with hits on the track, number of planes with hits exclusively on the track, significance of track curvature measurement, and reconstructed  $y$  defined as  $E_{shower}/E_\nu$  where  $E_{shower}$  is energy of the reconstructed hadronic shower. In all cases the MC distributions are tuned according to the results of Fig. 4 (see Sec. 3), and normalized by POT. The width of the bands for the MC distributions reflects the uncertainty associated with beam flux modeling.

- improved selection of  $\nu_\mu$  CC events and rejection of neutral-current (NC) backgrounds by use of a multivariate likelihood-based discriminant (PID) that includes more observables than previously used. The new selection takes advantage of correlations of the distributions of these observables with event length. The observables used are plotted in Fig. 1, and distributions of PID are shown in Fig. 2. We select events with  $PID > 0.85$ . The  $\nu_\mu$  CC selection efficiencies and NC background contamination fractions (in the null oscillation case for the FD) are plotted as a function of  $E_\nu$  in Fig. 3. Overall the efficiency for CC events has increased by approximately 1% with respect to the cut described in Ref [7], while the NC background has been reduced by more than a factor of two.

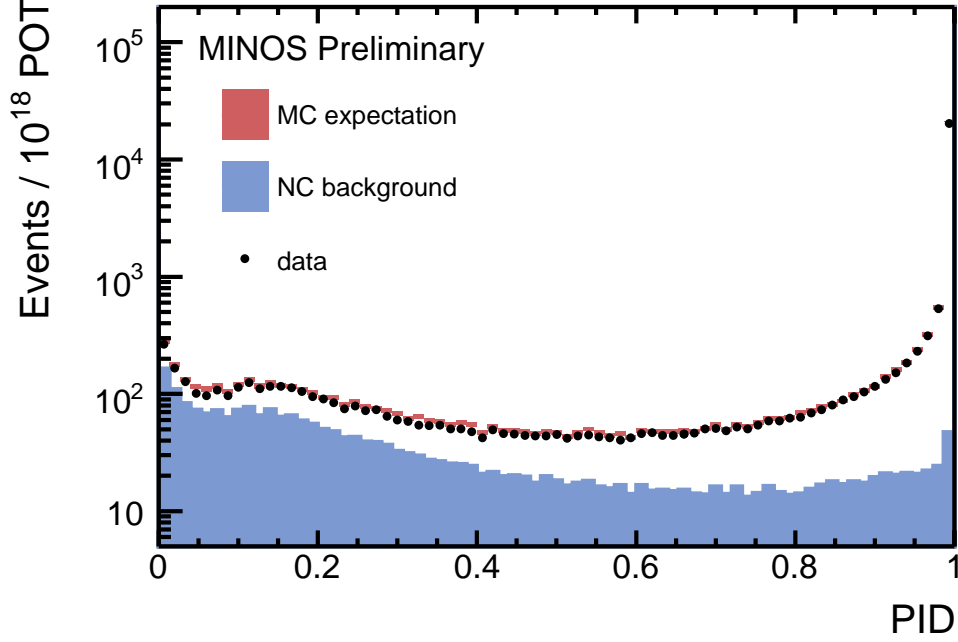


Figure 2: Distributions of the CC/NC separation discriminant (PID) for ND data (points) and MC (red bands) samples normalized by POT and weighted according to hadron production model tuning. CC candidates are required to satisfy  $PID > 0.85$ . The distributions for neutral current interaction events are shown represented by the blue shaded histograms.

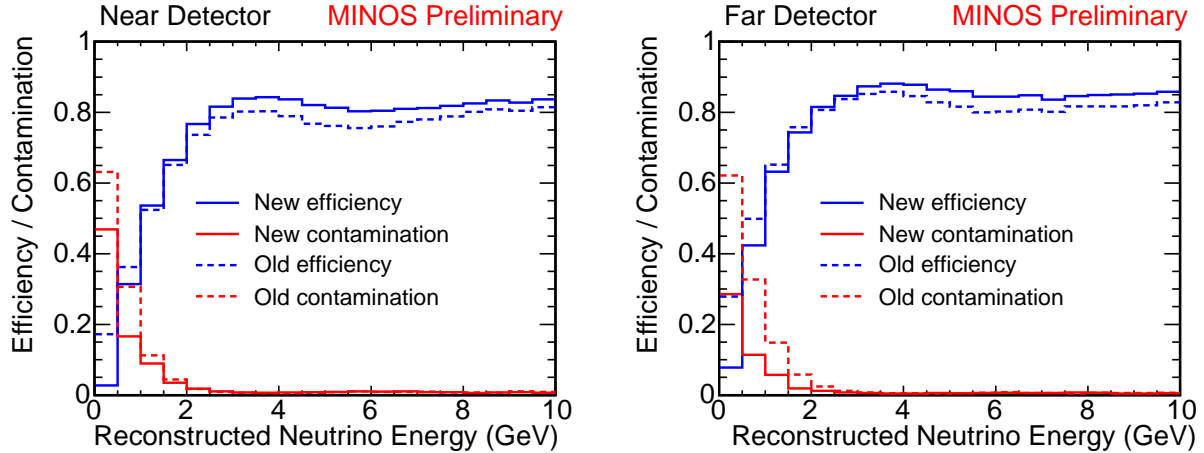


Figure 3: Selection efficiencies (blue) and NC background contamination fractions (red) for the  $\nu_\mu$  CC selection cut used in the new analysis for the ND (left) and FD (right). The corresponding curves from the selection cuts used in the previous analysis [7] are displayed by dashed lines. For the new analysis,  $\nu_\mu$  CC candidates in both ND and FD are defined by  $PID > 0.85$ , whereas in the previous analysis different cuts were used for the two detectors.

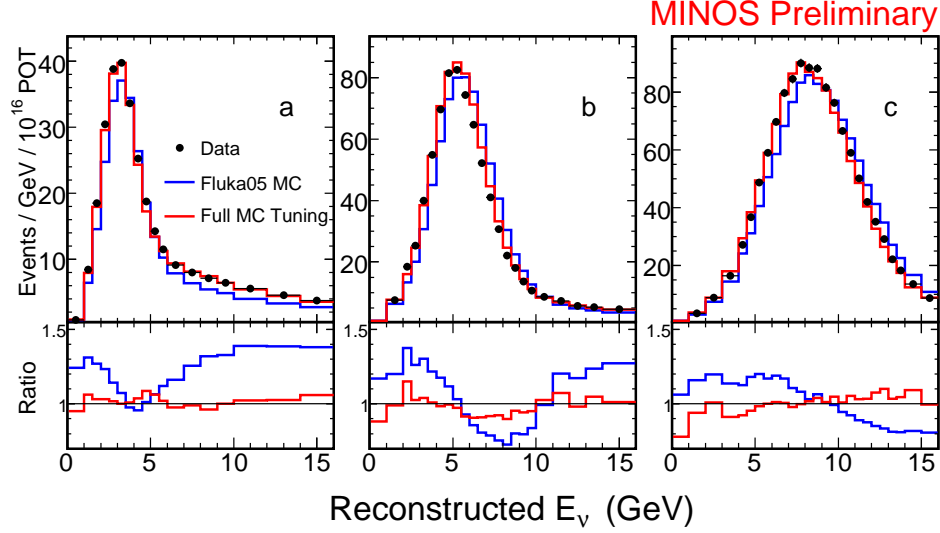


Figure 4: The ND reconstructed  $E_\nu$  spectra (points) for three of the seven beam configurations compared with MC spectra obtained before (blue) and after (red) the hadron production and beam tuning procedure. These configurations result from varying the target location ( $z$ ) and horn current ( $I$ ): (a) low-energy beam ( $z = -10$  cm, relative to the nominal position and  $I = 185$  kA), (b) medium-energy beam ( $z = -100$  cm,  $I = 200$  kA), and (c) high-energy beam ( $z = -250$  cm,  $I = 200$  kA).

### 3 Use of ND Data to Predict the FD $E_\nu$ Spectrum

As in Ref. [7], we derive an expected FD  $E_\nu$  spectrum by extrapolating the observed spectrum in the ND. We have employed an extrapolation scheme, denoted the “Beam Matrix” method [9], that is largely insensitive to mis-modeling of the neutrino flux and neutrino interaction cross-sections. To correct for higher order effects, we have tuned the hadron production model and other elements of the beam flux simulation and detector response to improve agreement of  $E_\nu$  and  $E_{\bar{\nu}}$  spectra from data taken under seven different beam configurations with the corresponding MC spectra. Fig. 4 shows the  $E_\nu$  spectra, comparing data with untuned (blue) and tuned (red) MC spectra for three beam configurations.

The null-oscillation FD  $E_\nu$  spectrum predicted by the Beam Matrix method is shown in Fig. 5, along with the corresponding predicted spectra from three other extrapolation methods used as cross-checks. Agreement between the methods is at the level of 4%.

## 4 Preliminary Results

### 4.1 FD Event Yields and $E_\nu$ Spectrum

From the Run-I and Run-IIa samples, we select 812 neutrino-like events with a reconstructed track in the FD fiducial volume, of which 563 satisfy  $\nu_\mu$  CC interaction selection (track quality, track charge sign and NC rejection) cuts. Some characteristics of the neutrino-like

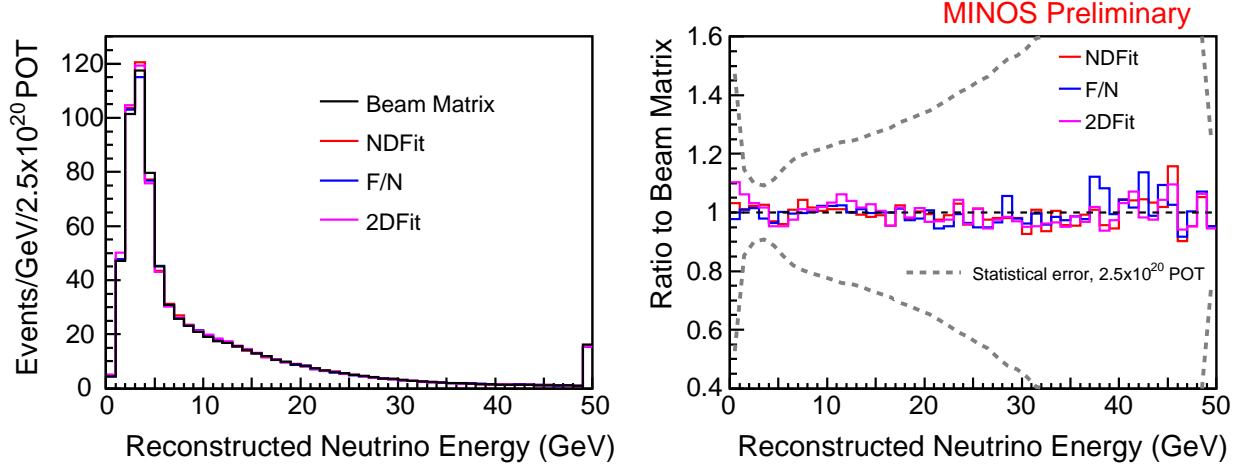


Figure 5: Left plot: predicted Far Detector reconstructed  $E_\nu$  spectra from four extrapolation methods (left) based on ND data; Right plot: ratios of spectra from cross-check extrapolation methods to the Beam Matrix prediction. The dashed line represents the expected statistical uncertainty on FD  $E_\nu$  spectrum bin contents for the current exposure. In both plots, the final bin at 49 GeV is an overflow bin, including events above 50 GeV as well.

events are shown in Fig. 6. Fig. 7 shows the  $E_\nu$  spectrum for the 563  $\nu_\mu$  CC interaction candidate events (points). Overlaid is the null-oscillation expectation (black histogram), totaling  $738 \pm 30$  events as inferred from the ND data, where the uncertainty is due to the FD/ND relative normalization systematic error. The expected contamination from the three main background sources is also shown: NC interactions (5.6 events),  $\nu_\tau$  CC interactions (0.8 events) and  $\nu_\mu$  CC interactions in the rock upstream of the FD or within the FD but outside the fiducial volume (1.7 events). The estimates for the latter two sources account for oscillation effects.

## 4.2 Oscillation Fit

We carried out a simultaneous fit of the oscillation-weighted predicted  $E_\nu$  spectra for Runs I and IIa to the corresponding observed FD spectra. The separation of Run-I and IIa FD data is motivated by differences observed in the corresponding ND spectra of  $\sim 7\%$  in the peak region owing to a difference of 1 cm in the NuMI target placement along the beam axis for the two running periods. In the fit the quantity  $\chi^2 = -2 \ln \mathcal{L}$ , where  $\mathcal{L}$  is the likelihood function, is minimized with respect to oscillation parameters  $\Delta m^2$  and  $\sin^2 2\theta$  as well as nuisance parameters  $\alpha$  incorporating the most significant sources of systematic uncertainty:

$$\chi^2(\Delta m^2, \sin^2 2\theta, \alpha) = \sum_i \{2(e_i - o_i) + 2o_i \ln(o_i/e_i)\} + \sum_j \frac{\Delta \alpha_j^2}{\sigma_{\alpha_j}^2},$$

where  $o_i$  represents the observed number of events in the  $i^{th}$  energy bin and  $e_i$  represents the corresponding oscillation-weighted expectation. Only values of  $\sin^2(2\theta) \leq 1$  were considered.

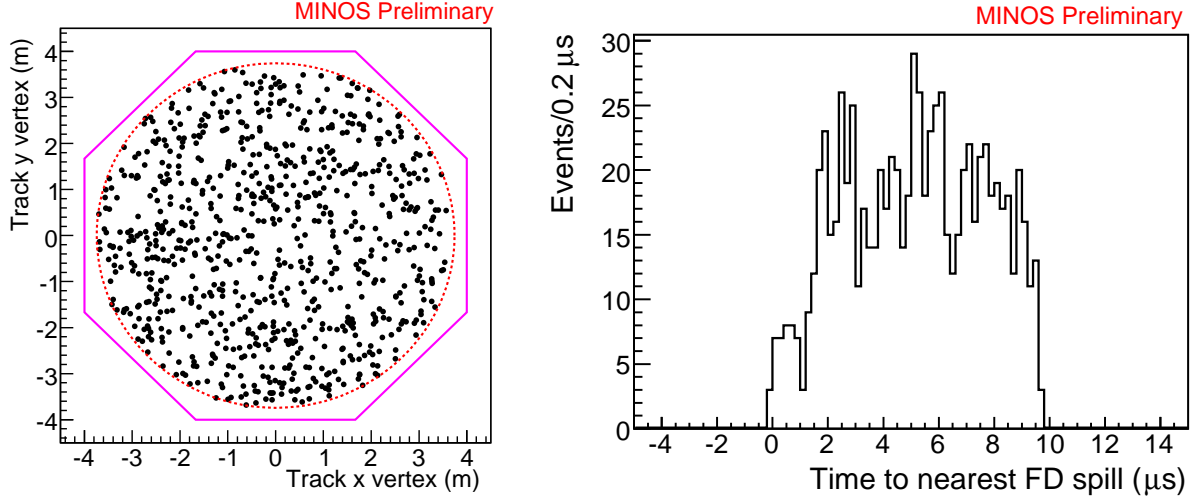


Figure 6: Left plot: the distribution of reconstructed interaction positions of neutrino-like events in the FD in the transverse plane. Shown also is the location of the radial fiducial volume cut. Right plot: the distribution of reconstructed times of FD neutrino-like candidates relative to the nearest NuMI beam spill time. The partial occupancy of the 0–1.5  $\mu\text{s}$  bins arises from various running conditions of the Main Injector, in which the NuMI spill length varied from 8.7–10  $\mu\text{s}$ , depending on other running experiments.

We included systematic uncertainties associated with the relative FD/ND normalization ( $\pm 4\%$ ), the hadronic shower energy scale ( $\pm 10\%$ ) and the NC background ( $\pm 50\%$ ).

The plots in Fig. 8 show the predicted FD spectrum weighted according to the best-fit oscillation parameter values (red) overlaid on the observed spectrum (points). The best-fit oscillation parameter values are:

$$\begin{aligned} |\Delta m_{32}^2| &= (2.38^{+0.20}_{-0.16}) \times 10^{-3} \text{ eV}^2/c^4 \\ \sin^2 2\theta_{23} &= 1.00_{-0.08}, \end{aligned}$$

corresponding to  $\chi^2 = 41.2$  for 34 degrees of freedom. The uncertainties represent 68% CL intervals, as estimated from the oscillation parameter value(s) giving an increase in  $\chi^2$  of one unit relative to the best-fit value when minimized with respect to all other parameters. The 90% CL lower limit on  $\sin^2 2\theta$  is found to be 0.84.

The values of  $\chi^2$  relative to the best-fit value are plotted separately as a function of  $\Delta m^2$  and  $\sin^2 2\theta$  in Fig. 9. Also shown are curves corresponding to the expected sensitivity, based on high-statistics Monte Carlo samples. When we relax the requirement  $\sin^2 2\theta \leq 1$ , the best-fit point moves into the unphysical region:  $\Delta m^2 = 2.26 \times 10^{-3} \text{ eV}^2/c^4$  and  $\sin^2 2\theta = 1.07$ , with  $\chi^2 = 40.9$ . This feature accounts for the observed trend that the obtained  $\Delta\chi^2$  curves are more restrictive than the corresponding sensitivity curves.

The 68% and 90% CL contours in oscillation parameter space are shown in Fig. 10. These are specified by the locus of parameter values giving  $\Delta\chi^2 = 2.30$  and 4.61, respectively,

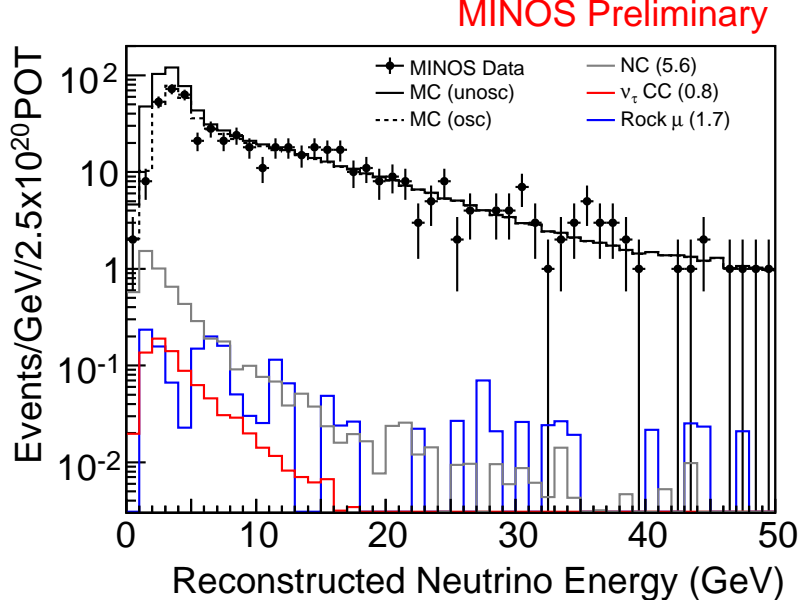


Figure 7: Reconstructed neutrino energy spectrum (points) from the Run-I plus Run-IIa Far Detector data sample. Overlaid is the Monte Carlo expectation, after tuning according to fits to the Near Detector data, without (solid black histogram) and with (dashed) best-fit oscillation weights. Shown also are the expected background contributions (accounting for oscillations) from  $\nu_\tau$  CC events, NC events and ‘rock muons’ from beam neutrino interactions occurring in the rock upstream of the detector or in the detector but outside the fiducial volume.

relative to the best fit point. We confirmed the coverage of these confidence intervals in a study employing the unified approach of Feldman and Cousins [10].

The new MINOS contours are compared with those from the published analysis of Run-I data [7] in the right plot in Fig. 10. The allowed region is shifted to lower values of  $\Delta m^2$  in the new analysis. Considering the two running periods separately, we find  $\Delta m^2 = (2.50^{+0.24}_{-0.20}) \times 10^{-3} \text{ eV}^2/c^4$  for Run-I and  $(2.22^{+0.44}_{-0.22}) \times 10^{-3} \text{ eV}^2/c^4$  for Run-IIa. The change in the absolute shower energy scale relative to the previous analysis (see Sec. 2) accounts for a systematic decrease of  $0.06 \times 10^{-3} \text{ eV}^2/c^4$  for both running periods relative to the published Run-I analysis. We have also carried out the Run-I analysis with the new neutrino interaction and event reconstruction software, but applying the same selection criteria as used in the previous analysis so as to have a greater overlap of FD  $\nu_\mu$  CC candidates, and obtain  $\Delta m^2 = 2.46 \times 10^{-3} \text{ eV}^2/c^4$ . We estimate the statistical significance of the deviation of this result from our published value (after accounting for the shower energy scale change) to be approximately two standard deviations based on the MC expectations for number of FD events lost and gained in migrating from the old to new track reconstruction codes.

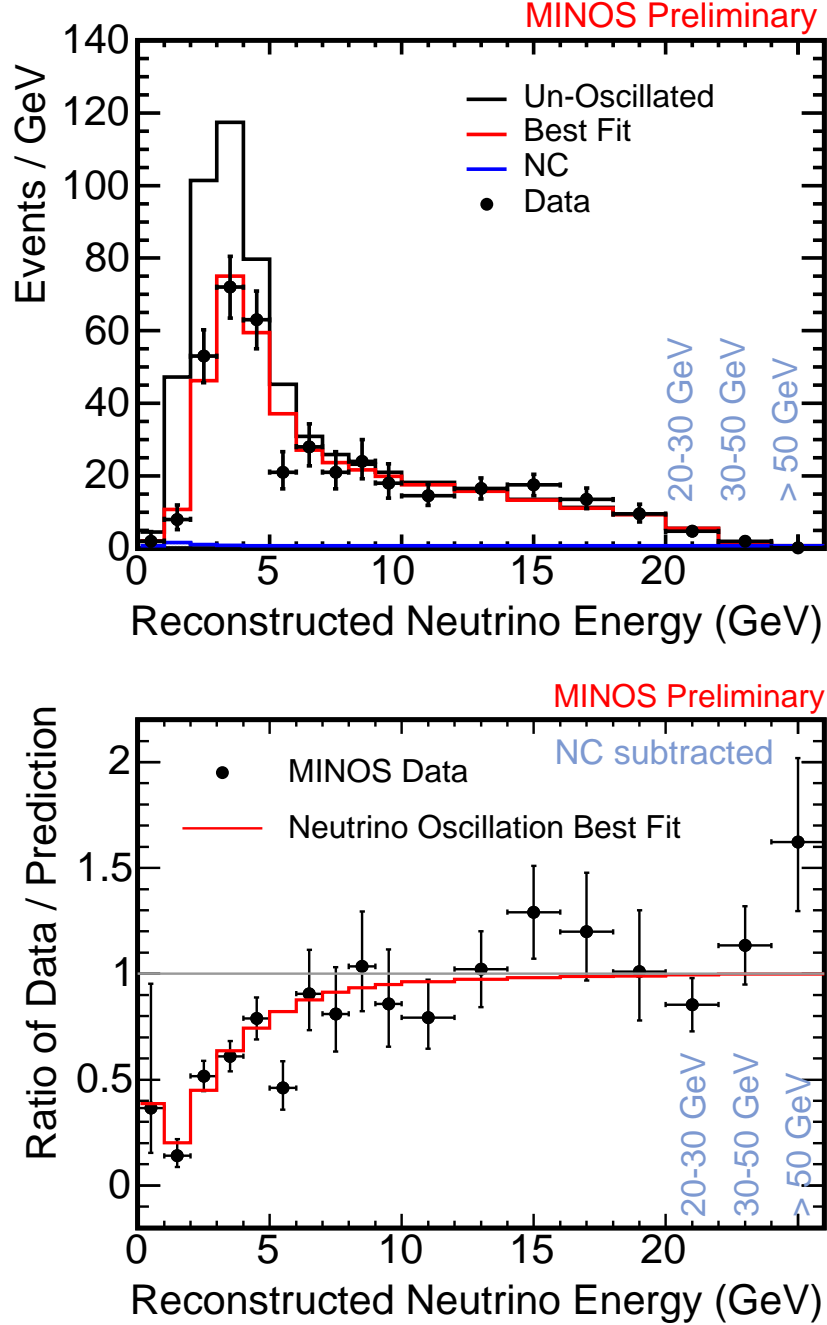


Figure 8: Top plot: the reconstructed  $\nu_\mu$  CC energy spectrum in the combined LE Run-I and IIa Far Detector data (points), with the null oscillation prediction overlaid (black histogram). Also shown are the oscillation-weighted prediction using best-fit parameters (red) and the expected NC background contribution (blue). The numbers of events in the final three bins, corresponding to energy ranges of 20–30, 30–50 and 50–200 GeV, have been scaled according to these bin widths. Bottom plot: the ratio of the NC-background subtracted FD spectrum to the null-oscillation prediction (points), with the best-fit oscillation expectation overlaid (red).

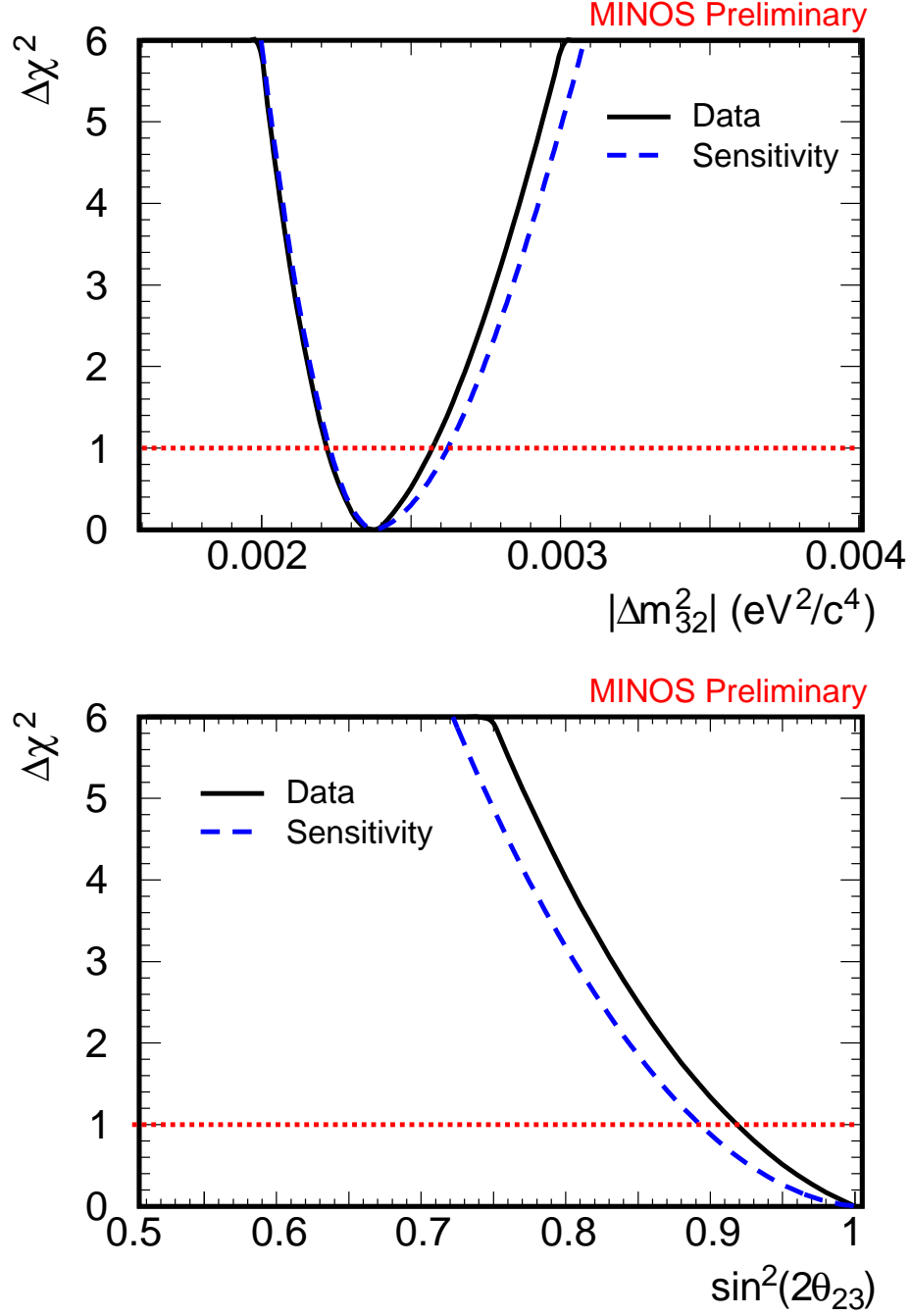


Figure 9: Plots of  $\chi^2$  versus  $\Delta m_{32}^2$  (top) and  $\sin^2 2\theta_{23}$  (right) for the analysis reported here (bottom). At each point  $\chi^2$  is minimized with respect to other fit parameters. The corresponding sensitivity are shown as dashed blue curves.

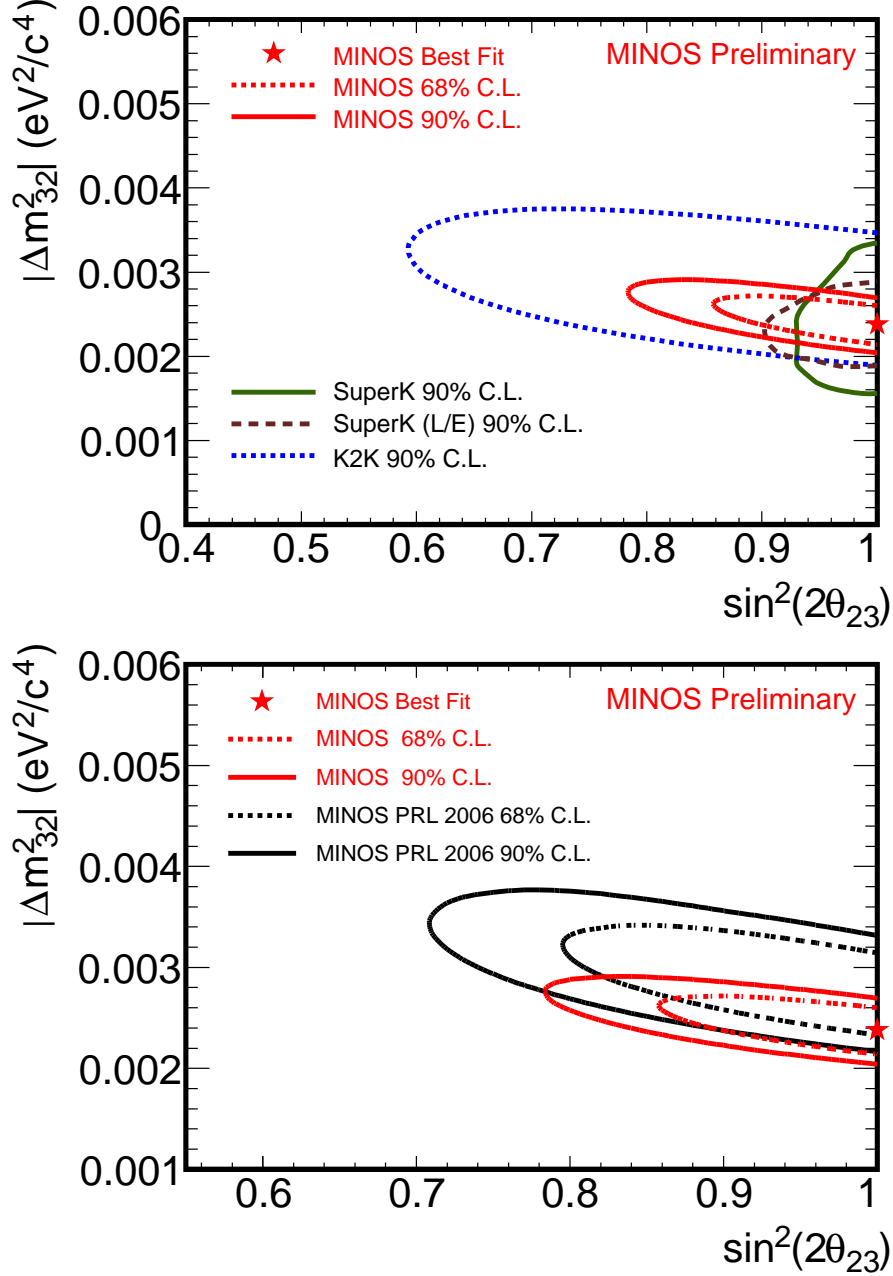


Figure 10: Top: The new preliminary MINOS best fit point (star) and the 68% and 90% CL contours (red) as determined according to  $\Delta\chi^2 = 2.30$  and 4.61, respectively. Overlaid are the 90% CL contours from the Super-Kamiokande zenith angle [3] and  $L/E$  analyses [2], as well as that from the K2K experiment [4]. Bottom: The new preliminary MINOS contours (red) are compared with the corresponding contours obtained in the original MINOS analysis of Run-I data [7].

## 5 Summary

We have reported preliminary results on  $\nu_\mu$  disappearance from the MINOS experiment based on an exposure corresponding to  $2.50 \times 10^{20}$  protons on target. The oscillation fit results are:

$$\begin{aligned} \left| \Delta m_{32}^2 \right| &= (2.38^{+0.20}_{-0.16}) \times 10^{-3} \text{ eV}^2/c^4 \quad (68\% \text{ CL errors}) \\ \sin^2 2\theta_{23} &> 0.84 \quad (90\% \text{ CL}), \end{aligned}$$

where the uncertainty includes both statistical and systematic sources. The value of  $\Delta m^2$  is smaller than but consistent with the previous MINOS result [7] of  $(2.74^{+0.44}_{-0.20}) \times 10^{-3} \text{ eV}^2/c^4$ . We are currently in the process of analyzing the full Run-I and Run-II dataset, with a total exposure of  $3.5 \times 10^{20}$  POT, of which  $3.25 \times 10^{20}$  POT is in the LE beam configuration and  $0.16 \times 10^{20}$  POT is in the HE configuration.

## 6 Acknowledgements

We thank the Fermilab staff and the technical staffs of the participating institutions for their vital contributions. This work was supported by the U.S. Department of Energy, the U.K. Particle Physics and Astronomy Research Council, the U.S. National Science Foundation, the State and University of Minnesota, the Office of Special Accounts for Research Grants of the University of Athens, Greece, and FAPESP (Fundação de Amparo à Pesquisa do Estado de São Paulo) and CNPq (Conselho Nacional de Desenvolvimento Científico e Tecnológico) in Brazil. We gratefully acknowledge the Minnesota Department of Natural Resources for their assistance and for allowing us access to the facilities of the Soudan Underground Mine State Park. We also thank the crew of the Soudan Underground Physics laboratory for their tireless work in building and operating the MINOS detector.

## References

- [1] K. S. Hirata *et al.* (the Kamiokande Collaboration), Phys. Lett. **B280**, 146 (1992);  
R. Becker-Szendy *et al.* (the IMB Collaboration), Phys. Rev. **D 46**, 3720 (1992);  
M. Ambrosio *et al.* (the MACRO Collaboration), Eur. Phys. J. C **36**, 323 (2004);  
W. W. W. Allison *et al.* (the Soudan 2 Collaboration), Phys. Rev. **D 72**, 052005 (2005).
- [2] Y. Ashie *et al.* (the Super-Kamiokande Collaboration), Phys. Rev. Lett. **93**, 101801 (2004).
- [3] Y. Ashie *et al.* (the Super-Kamiokande Collaboration), Phys. Rev. **D 71**, 112005 (2005).
- [4] M. H. Ahn *et al.* (the K2K Collaboration), Phys. Rev. **D 74**, 072003 (2006).
- [5] S. Kopp, “The NuMI neutrino beam at Fermilab,” in the Proc. of 2005 IEEE Part. Accel. Conf. (Knoxville, TN), May, 2005, Fermilab-Conf-05-093-AD and arXiv:physics/0508001.

- [6] D. G. Michael *et al.*, “The MINOS Detectors,” to be submitted to Nucl. Instrum. & Meth.
- [7] D. G. Michael *et al.* (the MINOS Collaboration), Phys. Rev. Lett. **97**, 191801 (2006);  
D. G. Michael *et al.* (the MINOS Collaboration), to be submitted to Phys. Rev. D.
- [8] **NEUGEN** version 3.5.0. See H. Gallagher, “The **NEUGEN** Neutrino Event Generator,” Nucl.Phys.Proc.Suppl.112:188-194,2002 as a reference for earlier versions.
- [9] M. Szleper and A. Para, hep-ex/0110001 (2001).
- [10] G. J. Feldman and R. D. Cousins, Phys. Rev. **D 57**, 3873 (1998).